

DELFT UNIVERSITY OF TECHNOLOGY

---

# Bi-threshold Mechanical Logic Gates for Cellular Automata based Intelligent Mechanical Metamaterials

---

*Authors:*

Eoinlee Bley (5216737)

*Supervisors:*

Dr. Davood Farhadi Machekposhti

Malte ten Wolde

in partial fulfillment of the requirements for the degree of

**Master of Science**

in Mechanical Engineering

September 24, 2023



## Abstract

## Contents

0.1	Elementary Cellular Automata Formalism . . . . .	2
0.2	Wolfram Numbering Scheme for ECA . . . . .	2
<b>1</b>	<b>Introduction</b>	<b>3</b>
<b>2</b>	<b>Results &amp; Discussion</b>	<b>3</b>
<b>A</b>	<b>Supplementary Material</b>	<b>12</b>

## 0.1 Elementary Cellular Automata Formalism

1. State Space:  $S = \{0, 1\}$
2. Neighborhood Configuration:  $N$   
 $N = (N_{-1}, N_0, N_1)$  where  $N_{-1}, N_0, N_1 \in S$
3. Rule Function:  $f : S^3 \rightarrow S$
4. Rule Set:  $R$
5. Cube Domain:  $D \subset \mathbb{R}^3$   
Each vertex directly corresponds to a neighborhood configuration  $N$ , and its state is
6. Separating Planes:  $P$   
Defined by a single normal vector  $\mathbf{n}$  and different offsets  $\{d_1, d_2, \dots, d_n\}$ .
7. Domain Classification Function:  $\Delta : D \rightarrow \{0, 1, 2, 3\}$   
 $\Delta(x) = \sum_{i=1}^n H(n_x \cdot x_x + n_y \cdot x_y + n_z \cdot x_z - d_i)$   
 $H(z) = \begin{cases} 0 & \text{if } z < 0 \\ 1 & \text{if } z \geq 0 \end{cases}$

## 0.2 Wolfram Numbering Scheme for ECA

In the Wolfram numbering scheme for Elementary Cellular Automata (ECA), the rule set  $R$  can be uniquely identified by a single integer, which is the binary representation of the output states for all possible neighborhood configurations. For Rule 110, the binary representation is formed by considering all 8 possible 3-cell neighborhood configurations, starting from 111 down to 000.

For example, in Rule 110, the corresponding output states for these configurations are 01101110. Here's how it maps:

Neighborhood Configuration	Output State	Binary Position (b)
111	0	$b_7$
110	1	$b_6$
101	1	$b_5$
100	0	$b_4$
011	1	$b_3$
010	1	$b_2$
001	1	$b_1$
000	0	$b_0$

So, the Wolfram number for Rule 110 is obtained by reading the output states from  $b_7$  to  $b_0$  as a binary number:  $01101110_2 = 110_{10}$ .

# 1 Introduction

- Mechanical computing uses deformation and mechanical motion for data storage and computation.
- Applicable in intelligent mechanical systems like soft devices, MEMS, and robotic materials.
- Limitation: Inefficient data exchange between memory and computing modules hampers performance.
- Logic gates realized through origami, buckled beams, and mechanical linkages.
- Signal propagation via mechanical, mechano-electronic, and mechanical-fluidic interfaces.
- Non-volatile mechanical memory exists but requires complex peripherals or intricate energy landscapes.
- Consideration: Cellular automata as a potential architecture to address data exchange bottleneck.

# 2 Results & Discussion

## Elementary Cellular Automata Formalism

Cellular automata (CA) are grid-based computational models where each cell evolves over time according to a rule set  $R$ . In Elementary Cellular Automata (ECA), the domain is one-dimensional and the state space is binary,  $S = \{0, 1\}$ . Each cell's future state is determined by its current state and those of its immediate neighbours.

Mathematically, for cell  $i$  at time  $t$ , the next state  $u_i^{t+1}$  is governed by a rule function  $f : S^3 \rightarrow S$ :

$$u_i^{t+1} = f(u_{i-1}^t, u_i^t, u_{i+1}^t)$$

With a binary state and 3-cell neighbourhood, there are  $2^8 = 256$  unique ECA rules. These are indexed from 0 to 255, following Wolfram's convention, detailed in subsection 0.2.

For example, Rule 110 is defined explicitly as:

$$f_{110} : \begin{aligned} &(0, 0, 0) \rightarrow 0, (0, 0, 1) \rightarrow 1, (0, 1, 0) \rightarrow 1, (0, 1, 1) \rightarrow 1, \\ &(1, 0, 0) \rightarrow 0, (1, 0, 1) \rightarrow 1, (1, 1, 0) \rightarrow 1, (1, 1, 1) \rightarrow 0 \end{aligned}$$

Consult [Figure 1A](#) for a graphical depiction of Rule 110's eight possible neighbourhoods and their respective output states. Also shown is the time evolution of the rule, starting from a single 'on' cell at the left edge of the domain.

## Hypercube Representation of Cellular Automata Rules

Consider a cube in  $\mathbb{R}^3$  as the domain  $D$ , with each vertex representing a unique neighbourhood configuration  $N = (N_{-1}, N_0, N_1)$ , where  $N_{-1}, N_0, N_1 \in \{0, 1\}$ . The cube's vertices are colored based on a rule function  $f : \{0, 1\}^3 \rightarrow \{0, 1\}$ , thereby geometrically realizing the Boolean truth table of an Elementary Cellular Automaton (ECA).

To introduce the concept of linear separability, consider separating parallel hyperplanes  $P$  defined by a normal vector  $\mathbf{n}$  and offsets  $\{d_1, d_2, \dots, d_n\}$ . These hyperplanes partition  $D$  into regions where the vertices share the same output state as determined by  $f$ .

We define a domain classification function  $\Delta : D \rightarrow \{0, 1, \dots, n\}$  as  $\Delta(x) = \sum_{i=1}^n H(\mathbf{n} \cdot \mathbf{x} - d_i)$ , where  $H(z)$  is the Heaviside step function. Each value of  $\Delta(x)$  corresponds to one of the  $n + 1$  regions formed by  $P$ .

Finally, a mapping function  $M : \{0, 1, \dots, n\} \rightarrow \{0, 1\}$  translates the region identifier  $\Delta(x)$  into the 'on' or 'off' state for each neighbourhood configuration. Refer to [Figure 1B](#) for a graphical representation of the cube and separating planes for Rule 110.

As shown in [Appendix A](#), most ECA rules are bi-planarly separable, i.e. they can be represented by two parallel planes.

The result of this formulation of 3-input Boolean functions as linearly separable regions in a cube is the observation that most 3-input Boolean functions can be represented by a pair of parallel planes. This means we can translate a complicated Boolean algebraic expression composed of several AND, OR, XNOR, etc., gates into a single bi-threshold perceptron gate.

The bi-threshold perceptron for this ECA context can be formally represented as:

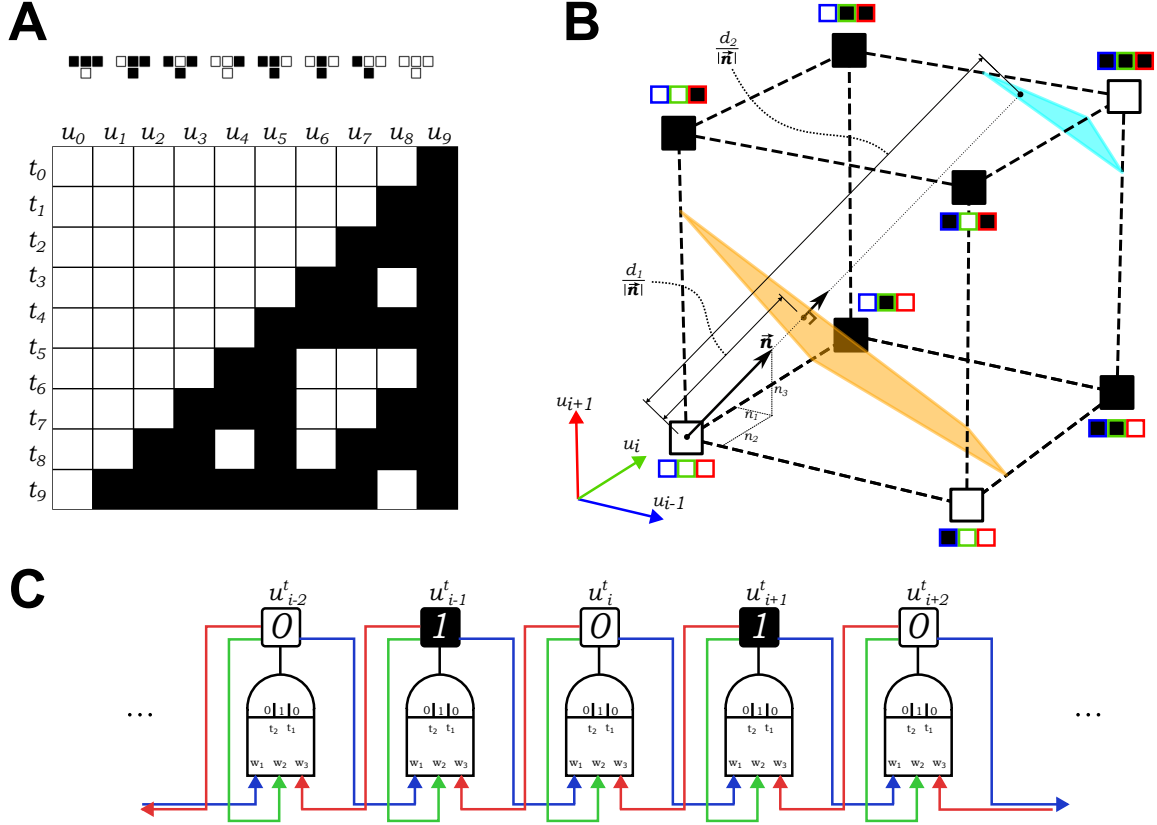


Figure 1: A. The transition rule and time evolution of the Rule 110 cellular automata. B. Cube representation Rule 110 with separating planes defined by normal vector  $\vec{n}$  and offset constants  $d_1$  and  $d_2$ . The red, green and blue colouring corresponds to left neighbour, middle, and right neighbour cells of the neighbourhood respectively. C. Bi-threshold gate representation of an ECA architecture.

$$f(N) = \begin{cases} 0 & \text{if } \sum_{i=-1}^1 w_i \cdot N_i > T_1 \\ 1 & \text{if } T_2 \leq \sum_{i=-1}^1 w_i \cdot N_i \leq T_1 \\ 0 & \text{if } \sum_{i=-1}^1 w_i \cdot N_i < T_2 \end{cases}$$

## Concept Mechanism

In light of the mathematical formalism presented, we introduce a conceptual mechanical metamaterial designed to embody the logic and behavior of Elementary Cellular Automata (ECAs). This metamaterial is constructed from an array of interconnected unit cells, each serving as a mechanical analog to the bi-threshold perceptron. The core of each unit cell is a tristable element, functioning as the decision-making component. The tristable element has three stable states, akin to the three regions separated by the two parallel planes in the cube of our geometric representation. This element is responsible for holding the output state of the cell, dictated by the weighted sum of its inputs.

Each unit cell is interconnected via coupling springs, which transmit mechanical signals between adjacent cells. The stiffness values of the coupling springs  $k_i$  act as the weights  $w_i$  in the bi-threshold perceptron equation. These values determine the force interactions and state transitions between adjacent unit cells. The tristable elements have multiple stable states, analogous to the regions separated by planes in the cube of our geometric ECA representation.

An input clock signal introduces a temporal dimension to the mechanical system, enabling dynamic state evolution similar to time-stepping in ECAs. This clock signal sets the computational cycle and synchronizes

the unit cells.

Thus, the mechanical properties of the springs and tristable elements correspond directly to the mathematical constructs of the bi-threshold perceptron, providing a means to implement ECA rules in a mechanical system. The specific embodiment of this concept is detailed in the following section.

## Unit cell design

The unit cell is designed to be planar and monolithic for scalability, operate under a single shared clock signal for synchronization, transmit forces between adjacent cells, hold state in the absence of input, and transition states according to neighboring conditions. Figure 2A depicts the unit cell and its key components: the tristable element in teal, the bistable element in purple, the signal transmission element in orange, and the input bifurcation element in dark blue. Coupling springs, coloured in red, green, and blue, link the tristable element out-of-plane to the bifurcation elements of adjacent unit cells. The configuration of each unit cell is fully defined by two displacements:  $d^t$  in the  $\hat{e}_1$  direction for the tristable element and  $d^b$  in the  $\hat{e}_1$  direction for the bifurcation element (due to the parallel links constraining rotational degrees of freedom). The input bifurcation element is so named because under actuation by an input clock signal  $\epsilon$ , its shuttle block will displace a distance  $\delta$  in one of two directions, pushing or pulling on the coupling springs according to the state of the unit cell, "on" or "off" respectively. In order for the the bifurcation element to bifurcate only due to the configuration of the bistable element and not the tristable element, the operation of the unit cell requires the coupling springs to be *tension-only* (Figure 2B). The details of this feature is elaborated in the next section.

The bistable element acts as a mechanical binary memory element for the unit cell, while the tristable element's two snapthrough force thresholds act as decision boundaries corresponding to the thresholds of the threshold gate, or the separating planes of the boolean function. The signal transmission and bifurcation elements facilitate the temporal clocking and informational interconnection of the unit cells.

A simplified pseudo-rigid body model of the unit cell is depicted in Figure Figure 2B. In this model, the contributions of numerous short-length flexure joints are aggregated into four torsional springs with angular stiffnesses ( $k_\alpha, k_\beta, k_\gamma, k_\theta$ ). These springs are subject to characteristic angular displacements ( $\alpha, \beta, \gamma, \theta$ ), which represent the angles of the tristable, bistable, signal transmission, and bifurcation links, respectively. The angles  $\alpha, \beta$ , and  $\gamma$  are part of a single-degree-of-freedom kinematic chain, while  $\theta$  and the input displacement  $\epsilon$  form another single-degree-of-freedom kinematic chain. The bistable element is simplified using symmetry and modeled as a single-link slider with torsional stiffness  $k_\beta$  and a reaction/support stiffness  $k_r$ . The transmission element is represented as a single link connecting the bistable element's shuttle block to a horizontal slider block. This link has a torsional stiffness  $k_\gamma$  and is guided by flexures with a support stiffness  $k_g$ . The signal transmission block is connected to the bifurcation element via a spring with stiffness  $k_s$ . This spring is attached at a point located a distance  $h$  from the anchor pivot of the bifurcation element.

Figure 2C shows the effect of the position of the tristable element on the behaviour of the bifurcation element under actuation.

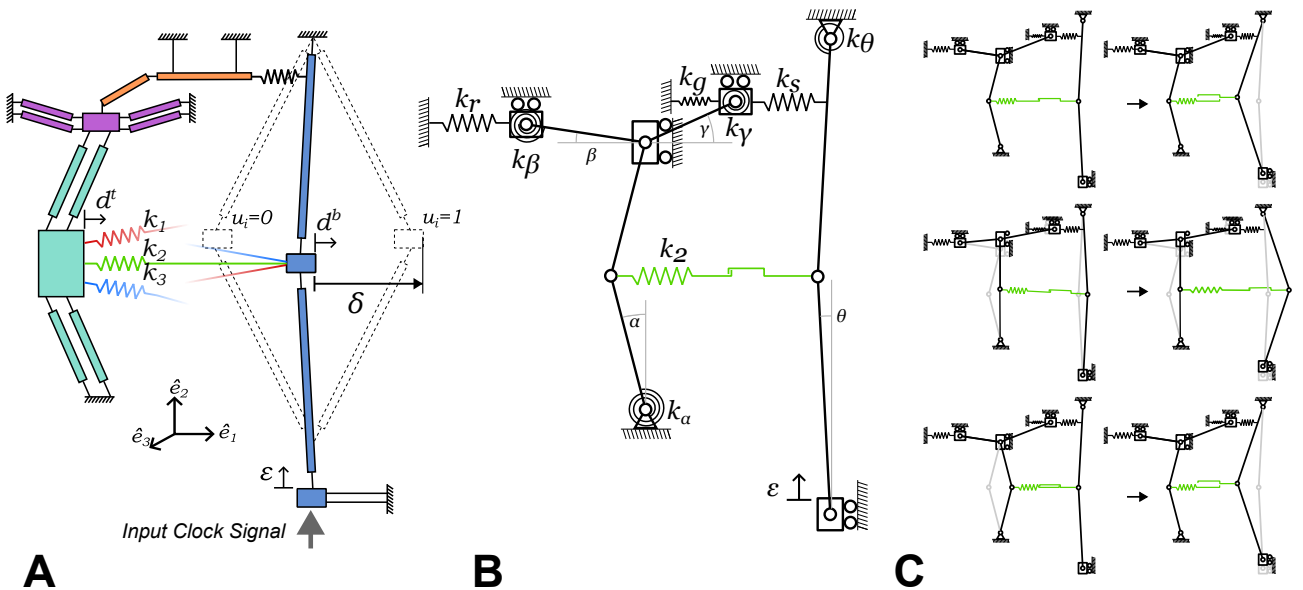


Figure 2: This is a figure.

## Working Principle/Kinetics

Figure 3A shows the theoretical force-displacement behaviour of the tristable element, graphing the reaction force on the tristable shuttle as a function of its horizontal displacement  $d^t$ . The three stable equilibria and corresponding configuration of the mechanism are shown. The specific behaviour is a function of all the stiffnesses and the chosen geometric dimensions and proportions of the mechanism.

The theoretical force-displacement behavior of the coupling tension-only springs is depicted in Figure 3B. Specifically, the spring behaves as a linear element with stiffness  $k_i$  when its elongation is positive. For negative elongation, the spring is slack, resulting in zero force. The stiffness  $k_i$  serves as a design parameter for selecting the specific ECA rule to be implemented.

Figure 3C illustrates a free-body diagram detailing the forces acting upon the tristable shuttle element. Here,  $F_r$  represents the total reaction force exerted by the tristable mechanism on the shuttle, while  $F_s$  denotes the cumulative force from all non-slack coupling springs. Equilibrium is achieved when the reaction and spring forces balance:  $F_r(d^t) = F_s(d^t, d^b)$ .

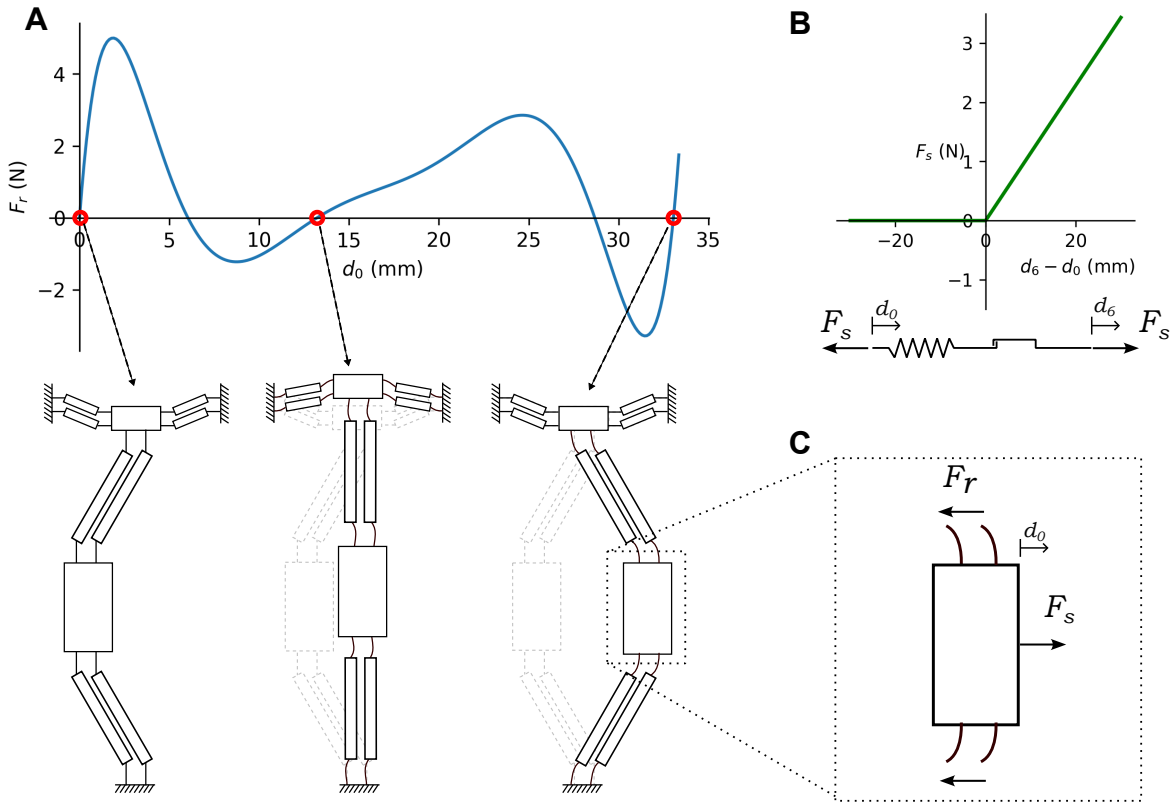


Figure 3: A. Force-displacement response of the three stable equilibria and corresponding configurations of the state element. B. Force-displacement response of the tension only spring

In Figure 4, the force-displacement behavior of the unit cell is depicted under varying conditions of coupling spring activations. When the bifurcation shuttle is fixed at a displacement  $\delta$ , denoted as  $d^b = \delta$ , the cumulative force from the activated coupling springs is plotted alongside the force-displacement curve of the tristable element,  $F_r(d^t)$ .

Equilibrium points emerge where these two force-displacement curves intersect and are represented as red dots on the difference plot. The equilibrium points correspond to the configurations where the cumulative force  $F_s$  from the coupling springs is equal to the reaction force  $F_r$  of the tristable element:  $F_r(d^t) = F_s(d^t, d^b)$ .

Now, let's address the "disappearance" of the equilibrium points. An equilibrium point "disappears" when the force-displacement line of the activated coupling springs no longer intersects with specific regions of the  $F_r$  curve—specifically, the regions around its local maxima. This occurs when the slope of the force-displacement curve for the activated springs, pivoting about the point  $d^b = \delta$ , not only fails to intersect but actually surpasses these local maxima of  $F_r(d^t)$ .

Create appendix for this derivation

generate pdf of this figure and edit axis labels for dt etc

In this context, snapthrough events happen as follows: the tristable element transitions from its current equilibrium state to an adjacent one depending on whether  $F_r < F_s$  or  $F_r > F_s$ . This transition is triggered when the equilibrium state corresponding to the current  $F_r$  and  $F_s$  values no longer exists. This mechanical action serves as the physical embodiment of the decision boundaries in the bi-threshold perceptron.

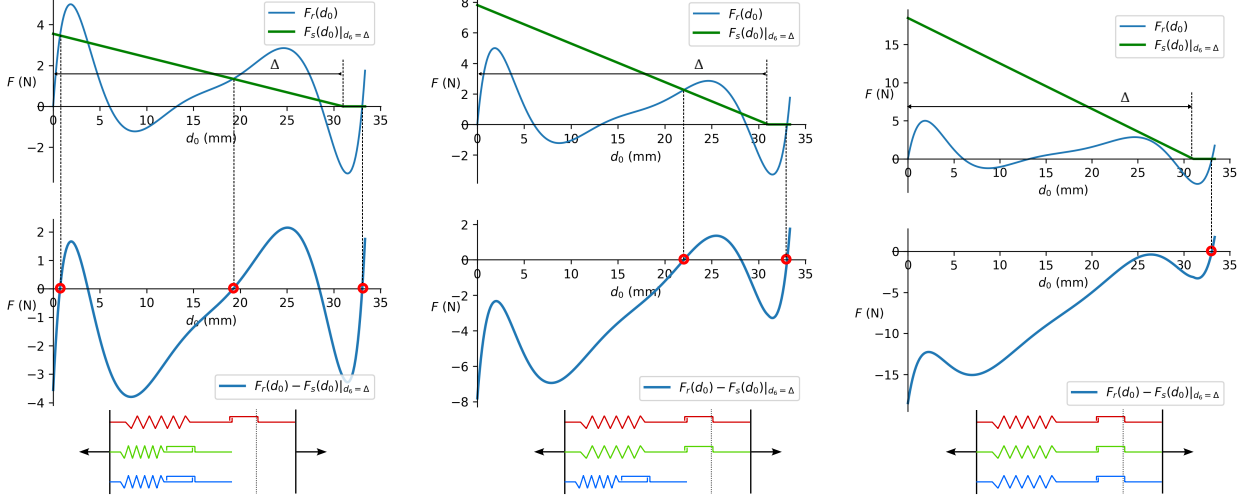


Figure 4: Force-displacement behavior with varying coupling spring activations. Equilibrium points, shown as red dots, emerge where the tristable element's reaction force  $F_r$  intersects with the cumulative spring force  $F_s$ . Equilibria disappear when the spring force curve, anchored at  $d^b = \delta$ , surpasses  $F_r$ 's local maxima, triggering a snapthrough event. This models the decision boundaries of a bi-threshold perceptron.

Recalling the mathematical formalism of ECA rules as bi-threshold perceptrons, we can now establish a direct correspondence between the mechanical and computational domains. In the bi-threshold perceptron model, the output state is determined by evaluating a weighted sum of inputs and comparing it against two threshold values  $T_1$  and  $T_2$ :

Here,  $w_i$  are the weights, and  $x_i$  are the input states from the neighborhood.

In the mechanical system, these weights  $w_i$  are analogous to the stiffness  $k_i$  of the coupling springs. The input states  $x_i$  correspond to the displacements  $d^b$  of the neighboring cells, a function of the states of their bistable elements. The thresholds  $T_1$  and  $T_2$  correspond to the critical effective stiffnesses of the cumulative active coupling springs at which the tristable element undergoes snap-through transitions. These critical effective stiffnesses are determined by the slopes of the lines that are tangent to the specific maxima regions on the  $F_r(d^t)$  force-displacement curve. These tangent lines are anchored at the point where  $d^b = \delta$  on the  $d^t$  axis.

## Parametric determination of ECA rule

Here we outline a parametric strategy for physically embodying a specific ECA rule, leveraging its geometric representation as parallel planes. The aim is to precisely calibrate the stiffness values  $k_i$  of the coupling springs and the maximum displacement  $\delta$  of the bifurcation element to manifest the desired ECA rule.

A pivotal insight is that modifying the bifurcation element's maximum displacement  $\delta$  alters the slopes of the lines tangent to the  $F_r(d^t)$  curve, as shown in Figure 5. These tangent lines are anchored at the point  $d^b = \delta$  on the  $d^t$  axis. This adjustment effectively varies the ratio between the bi-threshold perceptron's  $T_1$  and  $T_2$  values. Therefore, by selecting a specific  $\delta$ , we can control the orientation of the separating planes, aligning them with the desired ECA rule.

Subsequently, we can determine the coupling spring stiffnesses  $k_i$  that correspond to these plane orientations, thereby completing the physical embodiment of the selected ECA rule.

add reference instead of repeating equation



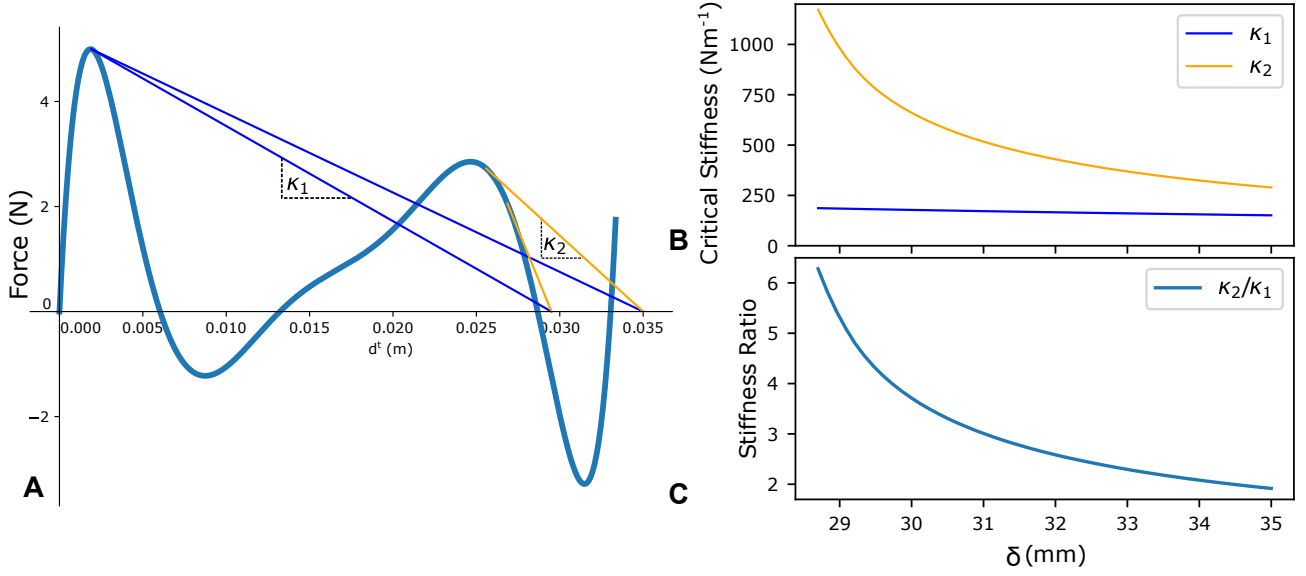


Figure 5: This is a figure.

### Implementation of Rule 110

To demonstrate the efficacy of this parametric design strategy, we implement Rule 110 in a physical prototype. The design process is as follows:

**Define Rule Characteristics** Each Elementary Cellular Automata (ECA) rule can be geometrically characterized by a normal vector  $\mathbf{n} = [n_1, n_2, n_3]$  and threshold values  $T_1$  and  $T_2$ . For example, for Rule 110,  $\mathbf{n} = [1, 2, 2]$  and  $T_1 = 1.5, T_2 = 4.5$ .

**Compute Critical Stiffness Ratio** The ratio of the threshold values,  $\frac{T_2}{T_1}$ , serves as a critical parameter in the design. For Rule 110,  $\frac{T_2}{T_1} = 3$ .

**Determine Bifurcation Displacement** The bifurcation displacement  $\delta$  corresponding to the critical stiffness ratio is determined by consulting Figure 5C. In the case of Rule 110,  $\delta \approx 31$  mm.

**Calculate Critical Stiffnesses** The critical effective stiffnesses  $\kappa_1$  and  $\kappa_2$  are obtained from Figure 5B, based on the selected bifurcation displacement  $\delta$ .

**Compute Coupling Spring Stiffness** The stiffness  $k_i$  of each coupling spring is then derived using:

$$k_i = \frac{n_i \times \kappa_1}{T_1}$$

The final mechanical parameters for a given ECA rule, such as Rule 110, are summarized in Table 1.

Parameter	Value	Units
$\kappa_1$	171.81	N/m
$\kappa_2$	515.39	N/m
$k_1$	114.54	N/m
$k_2$	229.08	N/m
$k_3$	229.08	N/m
$\delta$	31	mm

Table 1: Summary of Parametric Design Values for Rule 110

Figure 6 shows the equilibrium configurations of the tristable element for Rule 110 corresponding to the eight vertices of the cube representation. The effective stiffness of the coupling springs relative to the critical stiffnesses is shown for each neighborhood configuration

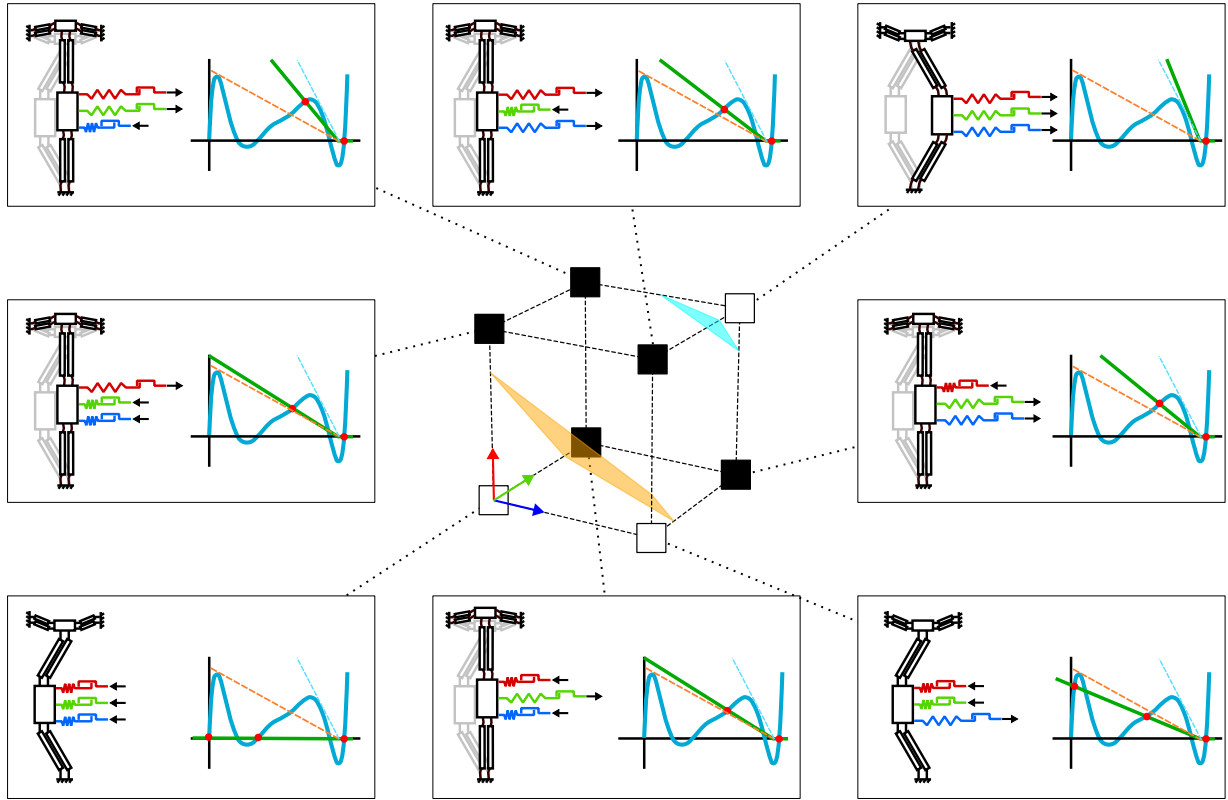


Figure 6: This is a figure.

Simulation

Compliant Embodiment

H

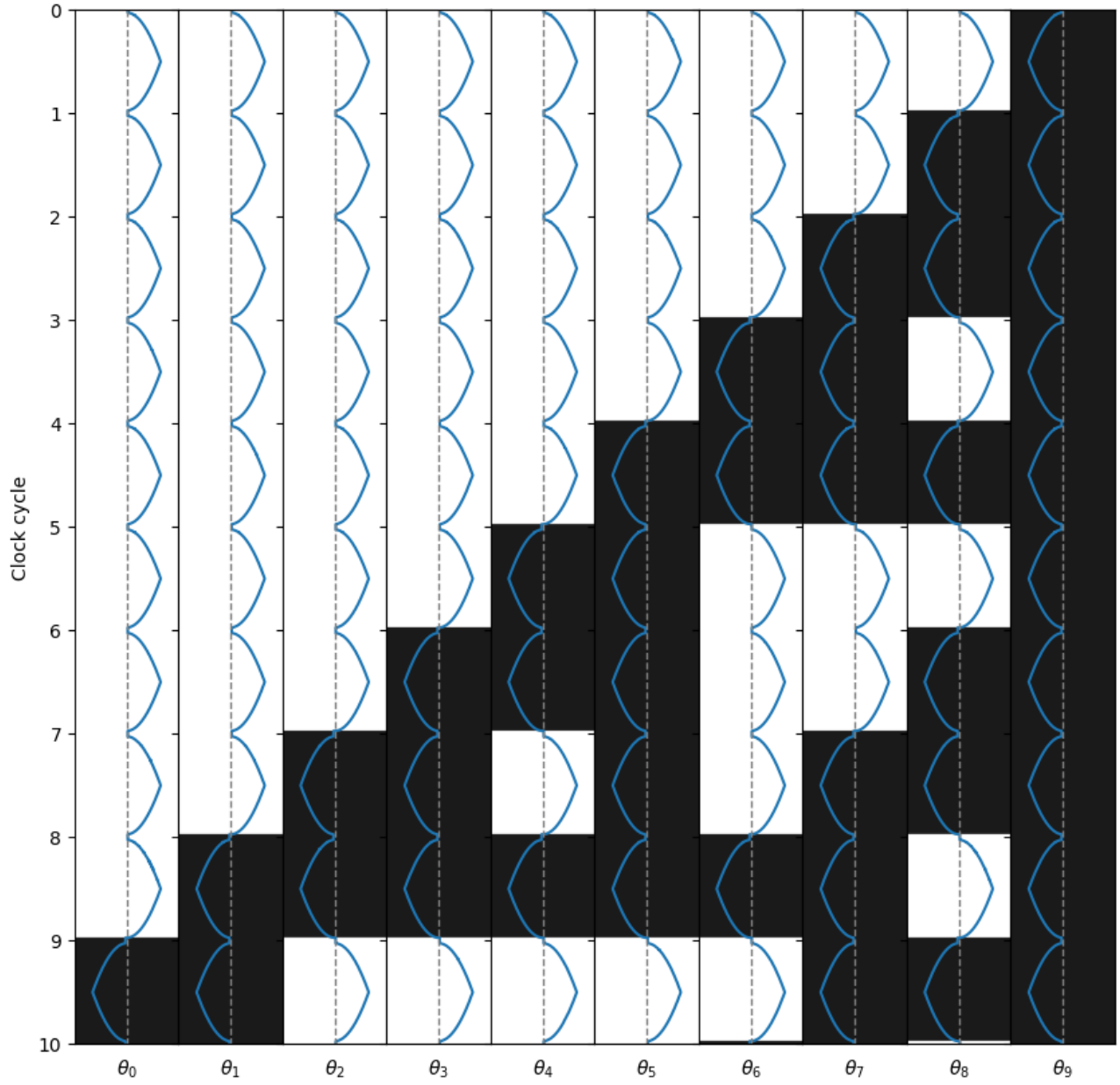


Figure 7: This is a figure.

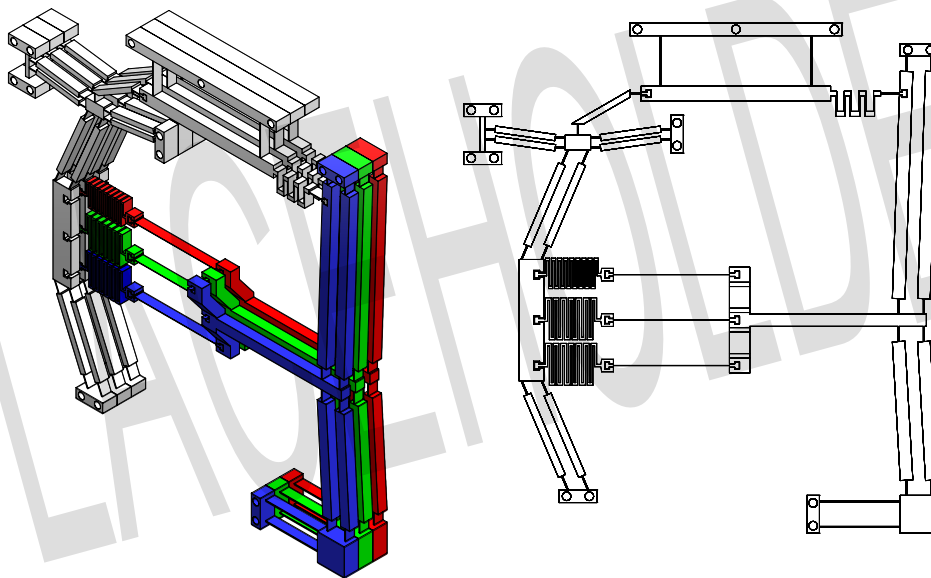


Figure 8: This is a figure.

## A Supplementary Material

### Bi-planar separability of ECA rules